efficient than SA and is also relatively easy to implement. SPSA requires only two measurements of the objective function regardless of the dimensions of the design space corresponding to the optimization problem and the cost of optimization decreases. Although SA and GA can avoid getting trapped in local optima, they require a large number of function evaluations and a long computation time to reach the optima. Future work to assess the performance of SPSA for constrained and unconstrained aerodynamic shape design studies will be carried out in the near future to establish the cost benefits and to investigate the extent to which SPSA offers comparative advantages over GA or SA for aerodynamic design optimization problems.

## References

[1]Wang, X., and Damodaran, M., "Comparison of Deterministic and Stochastic Optimization Algorithms for Generic Wing Design Problems," *Journal of Aircraft*, Vol. 37, No. 5, 2000, pp. 929–932.

[2]Spall, J. C., "Multivariate Stochastic Approximation Using a Simultaneous Perturbation Gradient Approximation," *IEEE Transactions on Automatic Control*, Vol. 37, No. 3, 1992, pp. 332–344.

[3]Raymer, D. P., *Aircraft Design: A Conceptual Approach*, AIAA Education Series, AIAA, Washington, DC, 1989.

[4]Spall, J. C., "An Overview of the Simultaneous Perturbation Method for Efficient Optimization," *Johns Hopkins Applied Physics Lab. Technical Digest*, Vol. 19, No. 4, 1998.

[5]Spall, J. C., "Implementation of the Simultaneous Perturbation Algorithm for Stochastic Optimization," *IEEE Transactions on Aerospace and Electronic Systems*, Vol. 34, No. 3, 1998, pp. 817–823.

[6]Deb, K., *Optimization for Engineering Design, Algorithms and Examples*, Prentice–Hall of India, New Delhi, 1998.

[7]Goldberg, D. E., *Genetic Algorithms in Search, Optimization and Machine Learning*, Addison Wesley Longman, Reading, MA, 1989.

# Lift Augmentation of a Low-Aspect-Ratio Thick Wing in Ground Effect

N. A. Ahmed* and J. Goonaratne†
*University of New South Wales, Sydney, New South Wales 2052, Australia*

## Nomenclature

| | | |
|---|---|---|
| $C_D$ | = | coefficient of drag |
| $C_L$ | = | coefficient of lift |
| $C_L/C_D$ | = | lift-to-drag ratio |
| $C_{\mathrm{MLE}}$ | = | coefficient of pitching moment about leading edge |
| $c$ | = | chord length |
| $h$ | = | true ground clearance |
| $Re$ | = | Reynolds number |
| $x_{\mathrm{CP}}$ | = | center of pressure measured from wing leading edge |
| $\alpha$ | = | angle of incidence |
| $\varepsilon$ | = | total solid and blockage correction factor |

## Introduction

IT is well known that in close proximity to the ground the aerodynamic characteristics of a wing change considerably, something that has come to be known as wing in ground effect. There have been several numerical studies to model the aerodynamic characteristics of airfoils under ground effect,[1–3] but reliable experimental data are somewhat limited.[4] Ground effect is important because it can modify the aerodynamic performance of an aircraft during landing and takeoff. It assumes even a greater importance in the design and operation of aircrafts that take off from and land on water and cruise in proximity to the water surface such as the wing-in-ground vehicles. Another possible application of such study lies in the design of naval vessel such as the high-speed catamaran where the vessel can be conceived to be a wing body at very low angle of incidence, and end plates extending beyond the wing bottom surface are used to represent its hulls. The aerodynamic lift would support part of the weight of the vessel and thus decrease the hydrodynamic drag by reducing the wetted area of the hulls. The aspect ratio of such a wing representing a high-speed marine vessel would, however, be low. Additional fixed angled flaps could, therefore, be used to boost the production of lift. With these considerations a wind-tunnel investigation of lift augmentation of a low-aspect-ratio wing of high thickness-to-chord ratio at a very low angle of incidence using ground effect, flaps and end plates was, therefore, carried out.

## Experiment

### Initial Considerations

The Reynolds number $Re$ for a catamaran (for example, the AMD K50 Sunflower) of length of approximately 80 m and operating at a speed of around 50 kn is about $1.35 \times 10^8$. Experimental and numerical studies[4,5] show that above $Re$ of $3.2 \times 10^5$, the aerodynamic performance characteristics of wing under ground effect remain virtually unchanged if the angle of attack is kept below 5 deg. A 1:50 scale model at a speed of 40 m/s and tested below angle of incidence 5 deg would give the test $R_N$ a value of around $3.6 \times 10^6$ for this study. This value was chosen for wind-tunnel testing to avoid Reynolds-number effect in the performance between the model and the full size of the craft.

Assuming a vessel clearance of 2 m from the water and again using the 1:50 scale, the minimum length with which the end plates under zero-deg flap condition could be extended was found to be 40 mm. The design of a ground board was considered necessary to represent a calm horizontal surface. Also, for aircrafts flaps are generally 20–40% of chord length, and they can operate at very high flap angles, 60 deg for example, and for short durations, usually during takeoff or landing. For this study, therefore, the flap length was considered to be much less than those used in aircrafts. Thus, taking a flap length of 12.5% of chord requires a flap of 168.75 mm in length, which was rounded off to 170 mm. This, along with 40-mm clearance for water surface gave a flap angle of 13.2 deg. A 0–10-deg range of flap angle was, therefore, considered adequate for this study.

### Test Facility

The $1270 \times 915$-mm closed-circuit wind tunnel fitted with a six-component balance of the aerodynamics laboratory of the University of New South Wales was used in the tests. The wind tunnel has a velocity range of 0–70 m/s and a turbulence intensity of 0.2%. A pitot-static tube with a Betz manometer was used to record the wind-tunnel speed upstream of the test model. Force and moment measurements from strain gauges were obtained from digital display on the control panel of the wind tunnel.

### Test Model

The upper surface cross-sectional profile of the wing body was generated through a consideration of a modified deck arrangements of an existing commercial high-speed catamaran while keeping the bottom surface flat. The top and middle decks were moved forward so that the maximum camber was obtained at 25% of chord from the leading edge. A schematic of this process is shown in Fig. 1. Using 1:50 scale, the chord, span, and height dimensions of the wing were worked out to be 1350, 180, and 230 mm, respectively. The maximum thickness-to-chord and aspect ratios of this wing then became 0.17 and 0.13, respectively.

The wing body was designed using the modeling package CATIA, and then NC milling codes were generated from CATIA facility. The

Received 10 September 2001; revision received 26 November 2001; accepted for publication 30 November 2001. 

*Senior Lecturer, Aerospace Engineering, Kensington.

†Graduate Student, Aerospace Engineering, Kensington.

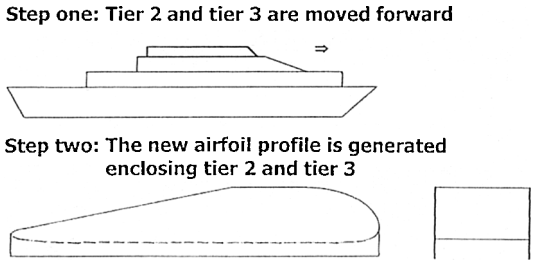


**Fig. 1 Design of airfoil shape.**

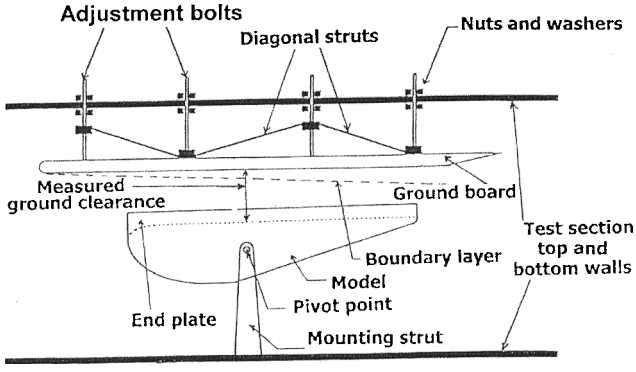


**Fig. 2 Schematic of the experimental setup.**

model was milled out of craft wood using the NC milling laboratory of the University of New South Wales.

### End Plates

The end plates were made with a 0.5-mm-thick aluminum sheet with a top surface contour matching that of the wing while the bottom surface was parallel to the wing bottom surface but extended below it. For flaps with higher angles, additional pairs of end plates were made. Thus all four pairs of end plates were made, which extended 40, 50, 65, 85, and 100 mm, respectively, below the bottom surface of the wing body.

### Flaps

A total of four flaps were made from craft wood. The length of each flap was 170 mm with angles of 0, 3, 6, and 10 deg for the four respective flaps.

### Ground Board

A ground board of 2400 × 1250 × 18 mm was used to simulate the ground effect. The leading edge of the ground board was elliptical in shape, and the trailing edge was tapered to ensure smooth and attached flow around it. The ground board was secured to the top of the wind-tunnel test section using Brooker bolts fastened by locknuts. Diagonal struts were used to prevent board vibration and buckling during wind-tunnel operation.

## Tests

### Experimental Setup

The wing model was held upside down in the wind tunnel on the mounting struts connected to the six-component balance. Figure 2 shows a schematic of the overall experimental setup.

### Determination of True Ground Clearance

A small hole was drilled through the middle of the ground board where the model was placed relative to the board. Inserting a small pitot probe through this hole, the velocity profile perpendicular to this board was measured. Using this velocity profile, the displacement thickness was calculated to be approximately 3.4 mm at this ground board location for the test $Re = 3.6 \times 10^6$. The displacement thickness was subtracted from the test setup ground height to obtain the true ground clearance.

### Measurements of Force and Moments

The six-component balance was calibrated for lift, drag, and pitching moments. The resulting calibration curves were then used for the determination of lift, drag, and pitching-moment coefficients.

### Blockage Correction

The model frontal area and test section were calculated as 0.0716 and 1.162 $m^2$, respectively. A quarter of the ratio of the total frontal area and test section area gave an approximate value for the total solid and wake blockage correction factor[5] $\varepsilon$, as 0.0154. The freestream velocity of the wind tunnel determined by the pitot-static

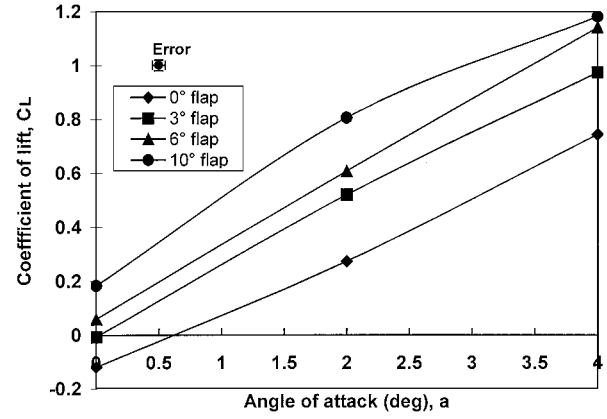


**Fig. 3a Variation of lift coefficient with angle of incidence ($Re$ = 3.6 × 10$^6$, $h/c$ = 0.035).**

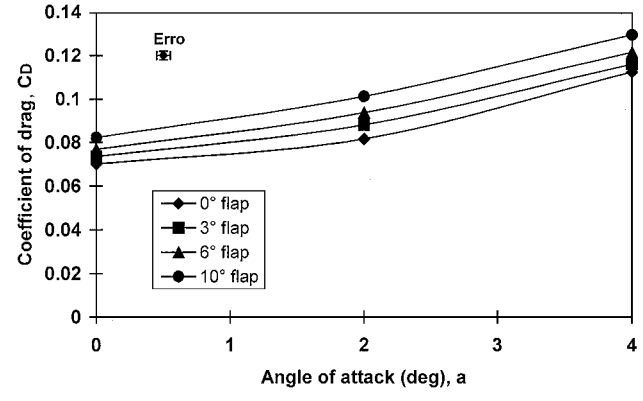


**Fig. 3b Variation of drag coefficient with angle of incidence ($Re$ = 3.6 × 10$^6$, $h/c$ = 0.035).**

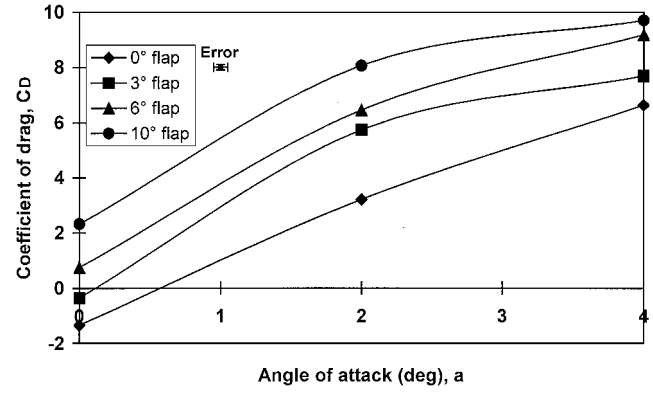


**Fig. 3c Variation of lift to drag ratio with angle of incidence ($Re$ = 3.6 × 10$^6$, $h/c$ = 0.035).**

probe was then multiplied by $(1+\varepsilon)$ or 1.0154 to correct for total blockage effect.[5]

### Error and Repeatability

The error associated with single sample measurements was calculated[6] and shown in each figure presented in this study. The repeatability of each test run was found to be within $\pm 1\%$.

## Results and Discussions

Figures 3a–3c show the variation of lift coefficient, drag coefficient, and lift-to-drag ratio, respectively, with angle of incidence in the range of 0–4 deg, at $Re = 3.6 \times 10^6$ and true ground clearance of $h/c = 0.035$. From Fig. 3a, as expected, the lift coefficient increases as angle of incidence increases and is further enhanced with higher angle of flap. A similar trend is also observed in Fig. 3b, where the drag coefficient is found to increase with higher angle of incidence and higher angle of flap. A more instructive picture, however, emerges in Fig. 3c, where the lift-to-drag ratio is found to increase with increase in the angle of incidence but which decreases with lower angle of flap. Also from Fig. 3c, it appears that the rise in the lift-to-drag ratio or the aerodynamic efficiency is more rapid in the 0–2 deg angle-of-incidence range. It was, therefore, decided to carry out the rest of the tests at the angle of incidence of 2 deg.

Figure 4a shows the lift coefficient variation with true ground clearance. The lift coefficient value decreases with increasing ground clearance. It appears that the maximum lift is generated between $0.02 < h/c < 0.03$. Also noticeable in this figure is the trend which was, as expected, that of increasing lift coefficient with increasing angle of flap.

The drag coefficient, however, in Fig. 4b remains virtually constant with increasing ground clearance for a particular flap angle.

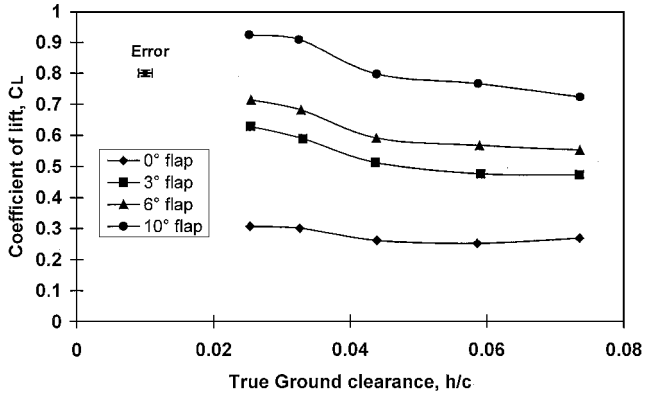


**Fig. 4a Variation of lift coefficient with ground clearance ($Re$ = $3.6 \times 10^6$, $\alpha$ = 2 deg).**

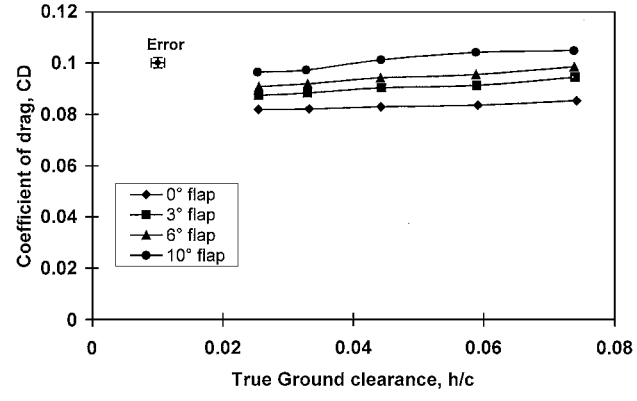


**Fig. 4b Variation of drag coefficient with ground clearance ($Re$ = $3.6 \times 10^6$, $\alpha$ = 2 deg).**

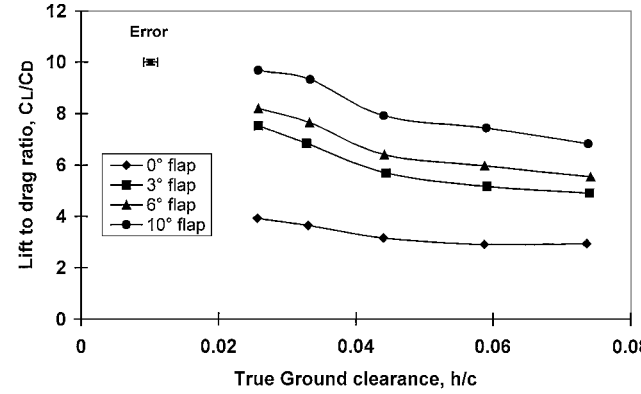


**Fig. 4c Variation of lift to drag ratio with ground clearance ($Re$ = $3.6 \times 10^6$, $\alpha$ = 2 deg).**

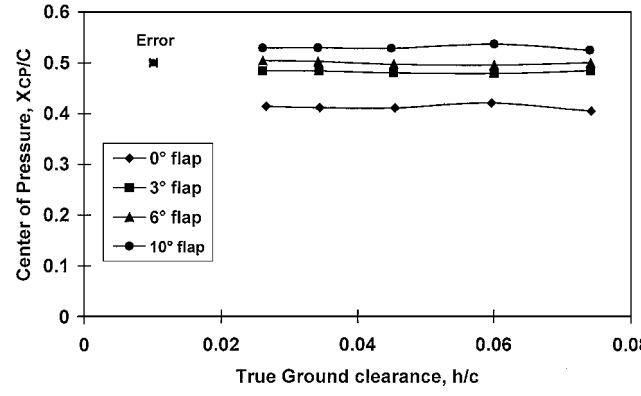


**Fig. 5 Variation of center of pressure with ground clearance ($Re$ = $3.6 \times 10^6$, $\alpha$ = 2 deg).**

Interestingly, the drag coefficient decreases with increasing flap angle. Consequently, in Fig. 4c the lift-to-drag ratio is found to be highest for the 10-deg flap operating between $0.02 < h/c < 0.03$. The maximum lift-to-drag ratio approaches a value of approximately 10.

Next, the movement of center of pressure measured from the wing leading edge was investigated. It can be seen in Fig. 5 that there is hardly any movement of the location of center of pressure with ground clearance. However, there is a clear change of the location of the center of pressure with changes in flap angle. For zero flap angle the center of pressure lies at approximately 40% of the chord behind the leading edge. When the flap is deflected by an angle of 3 deg, the center of pressure jumps to approximately 51% of chord length behind the leading edge. With further increases in flap angle to 6 deg, the movement is barely detectable, and center of pressure moves back slightly to around 50% of chord length behind the leading edge. With further increases in flap angle to 10 deg, the location of the center of pressure moves further towards the leading edge, to approximately 47% of chord length.

## Conclusions

The results of this study show that lift augmentation using flaps and end plates can prove beneficial to the design of crafts operating in close proximity to the ground. The hypothetical design and testing of a high-speed marine vessel suggest that the movement of the center of pressure decreases with increasing higher flap angles but at the expense of lower lift-to-drag ratio. However, it is worth recalling that the shape tested in this study had a very low aspect ratio and probably does not possess the most efficient aerodynamic shape. This was also true for end plates and flaps. There is, therefore, further scope to improve on the lift-to-drag ratio achieved in this study under ground effect by increasing the aspect ratio and

incorporating aerodynamically more efficient wing, flap, and end plate combinations.

## References

[1]Widnall, S. E., and Barrows, T. M., "An Analytic Solution for Two- and Three-Dimensional Wings in Ground Effect," *Journal of Fluid Mechanics*, Vol. 41, Part 4, 1970, pp. 769–792.

[2]Masuda, S., and Suzuki, K., "Simulation of Hydrodynamic Effects of a Two-Dimensional WIG Moving near the Free Surface," *Journal of the Society of Naval Architects of Japan*, Vol. 170, Dec. 1991, pp. 83–92.

[3]Nuhait, A. O., and Zedan, M. F., "Numerical Simulation of Unsteady Flow Induced by a Flat Plate Moving near Ground," *Journal of Aircraft*, Vol. 30, No. 5, 1993, pp. 611–617.

[4]Hayashi, M., and Endo, E., "Measurement of Flow Fields around an Airfoil Section with Separation," *Transactions of the Japan Society of Aero-Space Science*, Vol. 21, No. 52, 1978, pp. 69–75.

[5]Rae, W. A., Jr., and Pope, Alan, *Low–Speed Wind Tunnel Testing*, 2nd ed., Wiley, New York, 1984, pp. 371 and 421.

[6]Kline, S. J., and McClintock, F. A., "Describing Uncertainties in Single Sample Experiments," *Mechanical Engineering: The Journal of American Society of Mechanical Engineers*, Vol. 75, Jan. 1953, pp. 3–8.